The promotion effect of nitrous acid on aerosol formation in wintertime Beijing: possible contribution of traffic-related emission

Yongchun Liu[1*], Yusheng Zhang[1], Chaofan Lian[2,6], Chao Yan[3], Zeming Feng[1], Feixue Zheng[1], Xiaolong Fan[1], Yan Chen[2,6], Weigang Wang[2,6*], Biwu Chu[3,4], Yonghong Wang[3], Jin Cai[3], Wei Du[3], Kaspar R. Daellenbach [3], Juha Kangasluoma[1,3], Federico Bianch[1,3], Joni Kujansuu[1,3], Tuukka Petäjä[3], Xuefei Wang[6], Bo Hu[5], Yuesi Wang[5], Maofa Ge[2], Hong He[4] and Markku Kulmala[1,3*]

1. Aerosol and Haze Laboratory, Advanced Innovation Center for Soft Matter Science and Engineering, Beijing University of Chemical Technology, Beijing, 100029, China

2. State Key Laboratory for Structural Chemistry of Unstable and Stable Species, Beijing National Laboratory for Molecular Sciences, Institute of Chemistry, Chinese Academy of Sciences, Beijing 100190, China

3. Institute for Atmospheric and Earth System Research/Physics, Faculty of Science, University of Helsinki, P.O. Box 64, FI-00014, Finland

4. State Key Joint Laboratory of Environment Simulation and Pollution Control, Research Center for Eco-Environmental Sciences, Chinese Academy of Sciences, Beijing, 100085, China

5. State Key Laboratory of Atmospheric Boundary Layer Physics and Atmospheric Chemistry, Institute of Atmospheric Physics, Chinese Academy of Sciences, Beijing, 100029, China

6. University of Chinese Academy of Sciences, Beijing 100049, PR China

Supplement information

Non-refractory $PM_{2.5}$ (NR-$PM_{2.5}$) measurement. Concentration of NR-$PM_{2.5}$ was measured with a ToF-ACSM (Aerodyne Co. Ltd., USA). The operation protocol and the configuration of ToF-ACSM has been described well in previous work [1]. Namely, $PM_{2.5}$ particles from the inlet were focused by a $PM_{2.5}$ aerodynamic lens [2], and then vaporized by a standard vaporizer heated at 600 °C followed by electronic ionization (EI, 70 eV). The non-refractory components including chloride, nitrate, sulfate, ammonia and organics were measured using a time-of-flight mass spectrometer with unit mass resolution (UMR). The concentrations of the above species were calculated based on the measured fragments signals, the signal ions (SI), the fragment table, the measured ionization efficiency (IE) of nitrate and the corresponding relative ionization efficiency (RIE) for sulfate, chloride, ammonia and organics. IE calibration of nitrate was performed using 300 nm dry NH_4NO_3 every month during this observation study.

VOCs measurement. VOCs were measured using a Single Photo Ionization Time-of-flight Mass spectrometer (SPI-ToF-MS 3000R, Hexin Mass Spectrometry). 0.8 L min^{-1} of filtered air was sucked from the whole sampling tube and heated to 80 °C in the inlet. VOCs were selectively enriched continuously through a polydimethylsiloxane (PDMS) membrane, and then ionized by VUV light (10.5 eV) with a deuterium lamp. The concentration of VOCs was determined with the time-of-flight mass spectrometer (ToF-MS) based upon external standard curves of PAMS and TO-15 standard gases (Linde Electronics & Specialty Gases, USA). VOCs with m/z from 40 to 300 were recorded with 3 min of time resolution, while hourly averaged concentration were reported in this work. Calibration was performed every week.

HONO measurement. HONO in ambient air directly sampled from the window of the laboratory was absorbed by a solution containing 0.06 mol L^{-1} sulfnilamide in 1 mol L^{-1} HCl, and then transformed into an azo dye by *N*-(1-naphthyl) ethylene-diaminedihydrochloride (0.8 mml L^{-1}). The azo dye was pumped into Teflon absorption cells (Liquid Core Waveguide, LCW) and detected by a mini-spectrometer with a diode array detector (Ocean Optics, SD2000). The HONO concentrations was obtained by subtracting the calibrated signal of the second coil from the first coil using external nitrile standard solutions. Zero point calibration was performed every day using scrubbed zero air [3].

Photolysis rate constants of HONO and O_3. Photolysis rate constants of NO_2(J_{NO2}), HONO(J_{HONO}) and O_3(J_{O3}) for clear sky conditions were calculated according to the solar zenith angle and the location using a box model (FACSIMILE 4). NO_2 photolysis sensor (J_{NO2}, Metcon) was unavailable during our observation study. However, it was available in from Aug 17 to Sep 16, 2018. Calibration function between the measured UVB light intensity and J_{NO2} from Aug 17 to Sep 16, 2008 was established to correct the influence the climatological O_3 column, aerosol optical depth and cloud cover on surface UV light intensity. As shown in Figure S8, the model well predicted the J_{NO2}. Then the J_{NO2} during this campaign study was predicted using the model. We further confirmed the calculated J_{NO2} by comprising the OH concentration estimated by the J_{O1D} according to the equation (c_{OH}=$J_{O1D}\times 2\times 10^{11}$ molecules cm^{-3}) [4] and the measured OH concentration at Huairou, which is 60 km northeast from BUCT, form Jan 11 to

Mar 10, 2016. As shown in Figure S8C, the estimated diurnal curve of OH is comparable with that measured at Huairou.

Supplementary figures

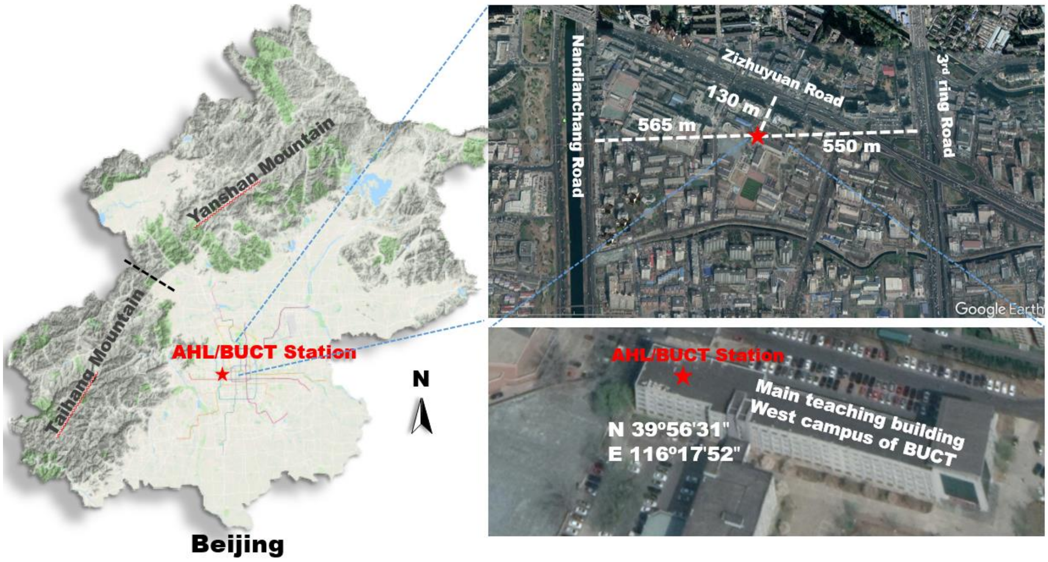

Figure S1. Location of AHL/BUCT observation station. The map was made from Wemap and © Google Earth.

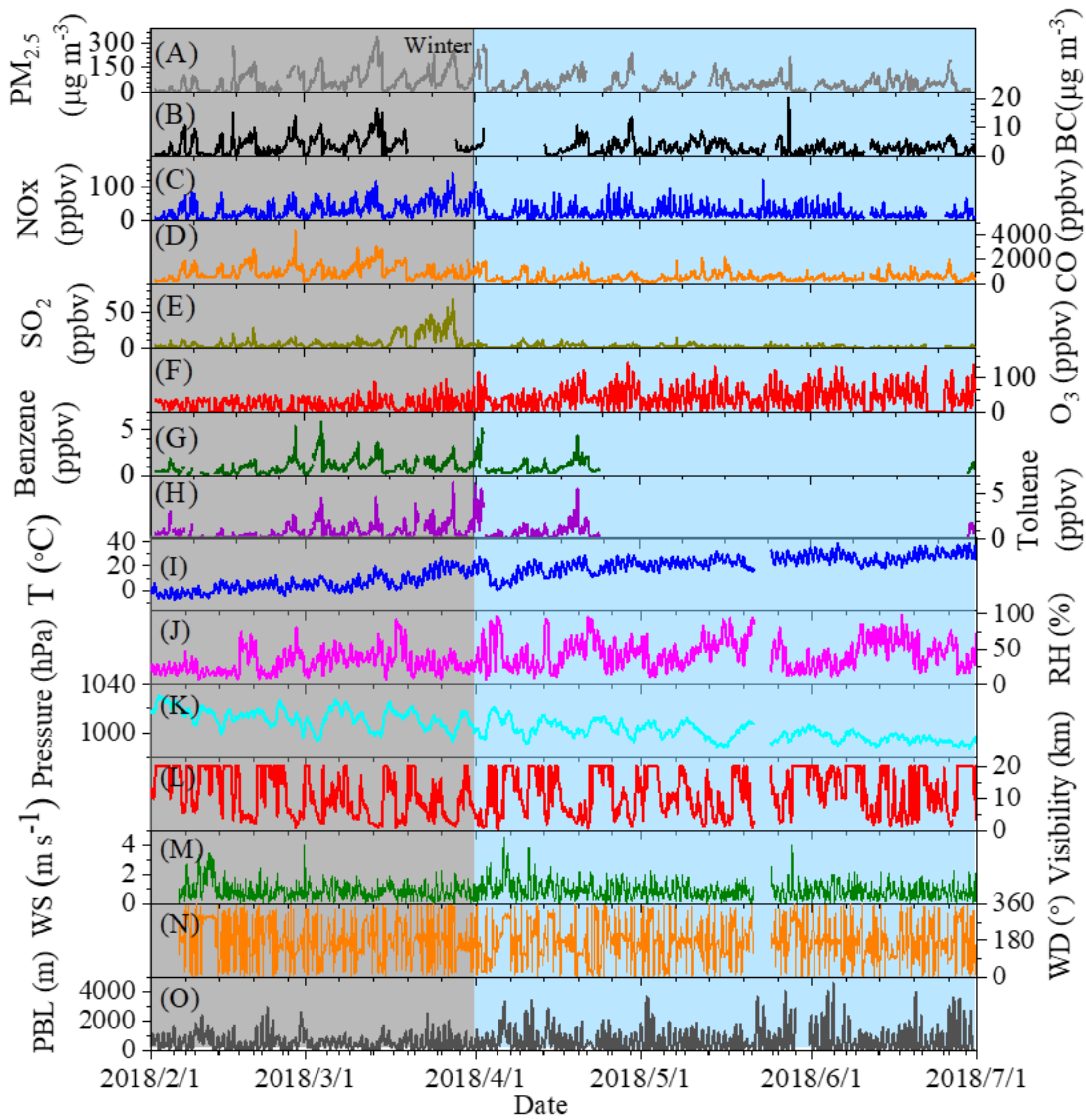

Figure S2. Hourly averaged (A)-(H) concentration of pollutants and (I)-(O) meteorological parameters from Feb 1 to Jun 30, 2018. $PM_{2.5}$ concentration data were obtained from surrounding National Environmental Monitoring Centre of China. PBL data were obtained from the NOAA Hysplit model.

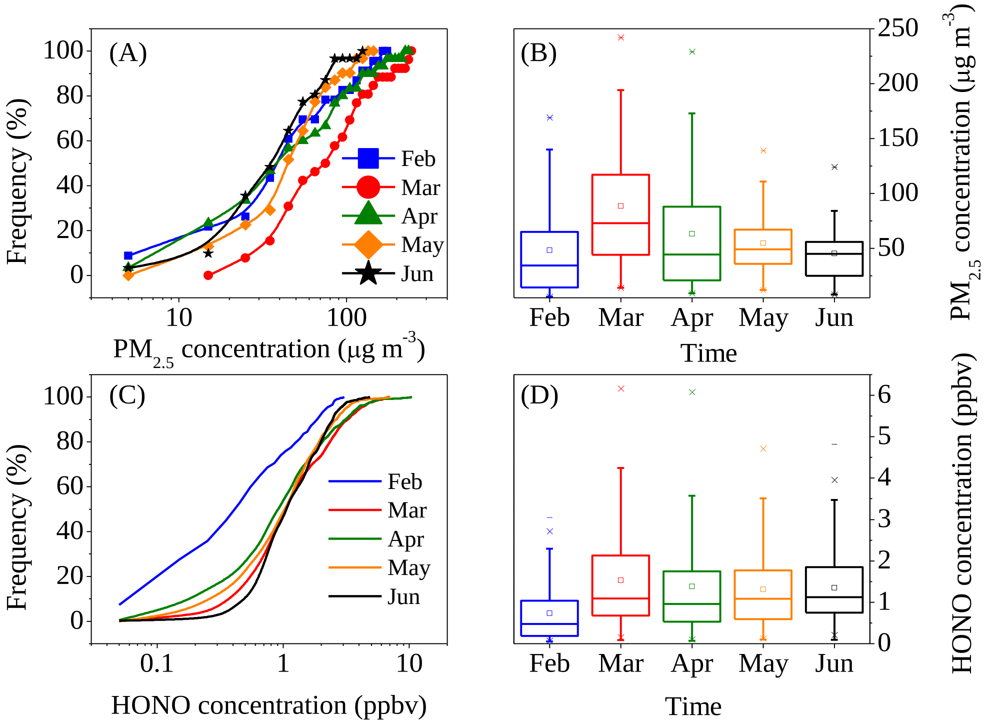

Figure S3. The monthly cumulative frequency of $PM_{2.5}$ and HONO and the monthly mean concentration of $PM_{2.5}$ and HONO.

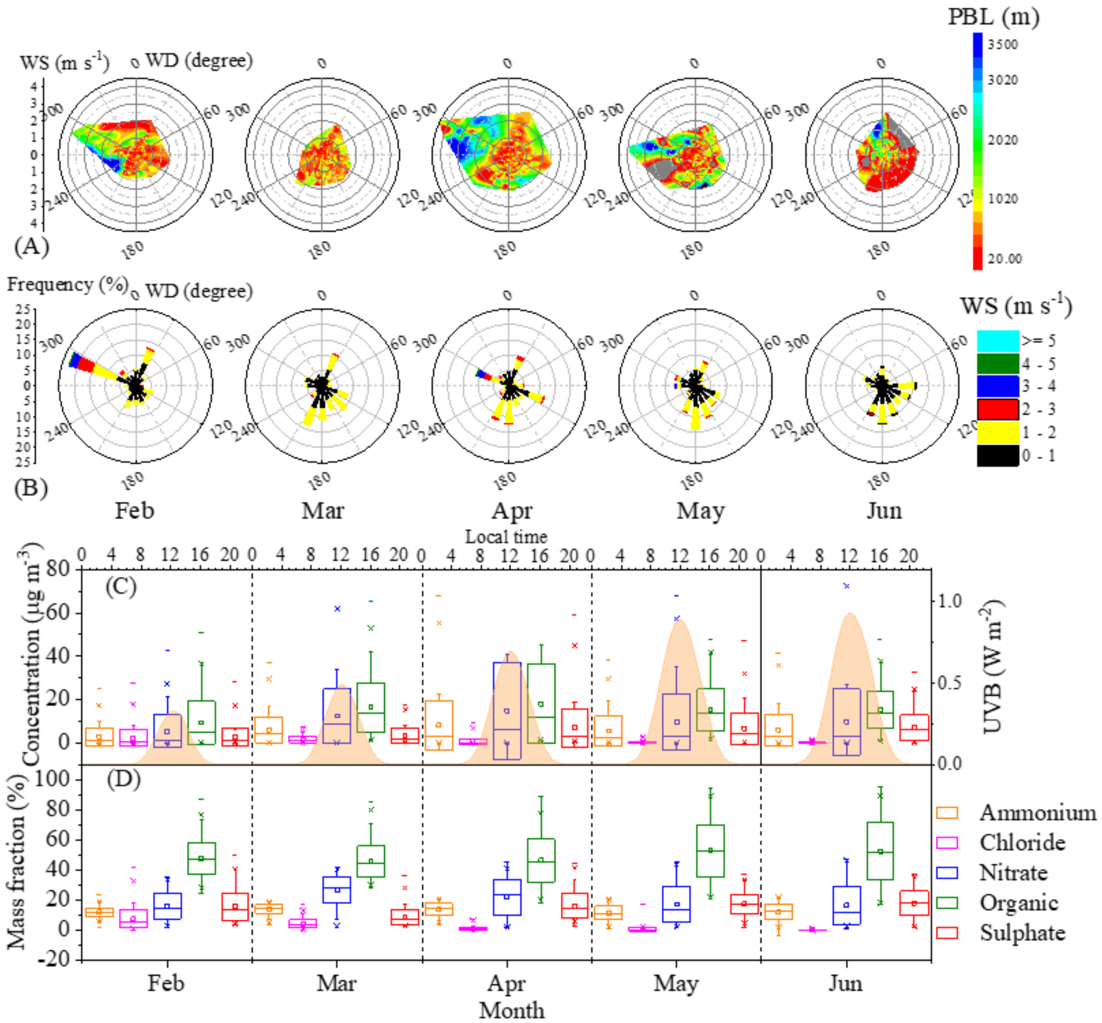

Figure S4. (A)-(B) monthly Windrose-PBL plots, and monthly averaged (C) UVB intensity, mass concentration and (D) fraction of individual component in NR-$PM_{2.5}$ composition from Feb to Jun, 2018.

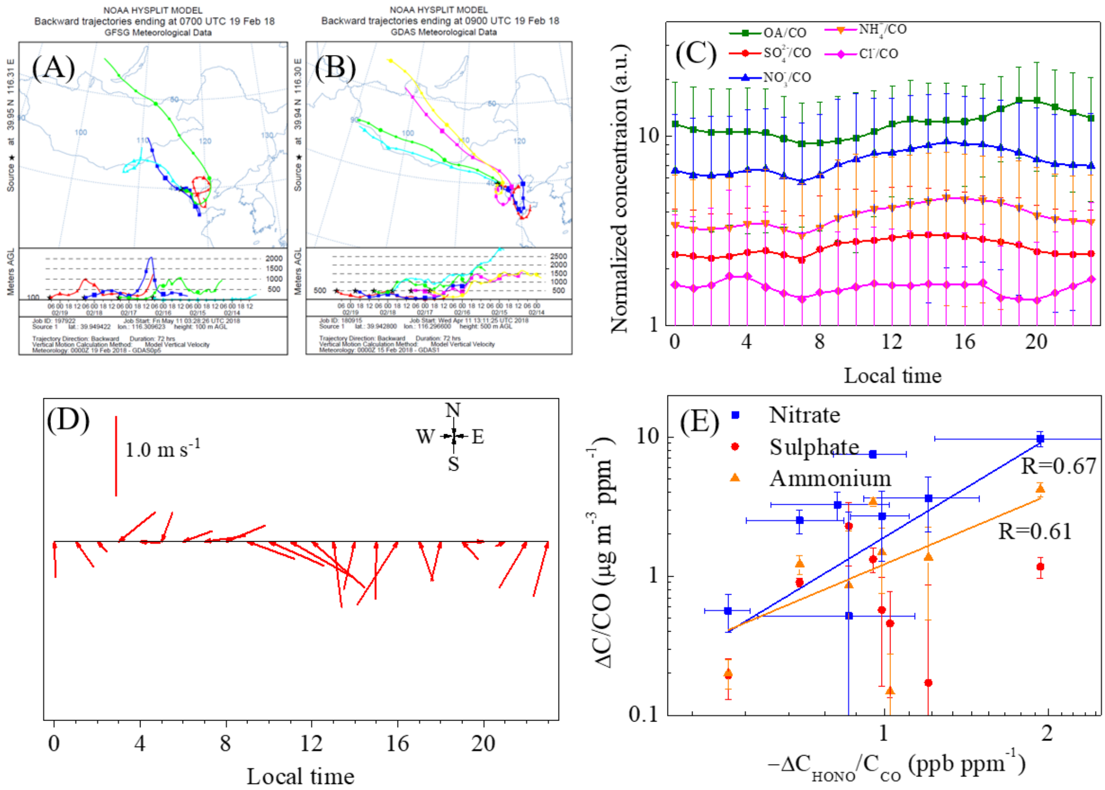

Figure S5. Transport of air mass during Chinese New Year based on back trajectory analysis (A) at 100 and (B) 500 m height; (C) Diurnal variation of NR-$PM_{2.5}$ normalized to CO concentration from Feb 1 to March 31; (D) Hourly averaged wind speed variation in the 12th episode; (E) Correlation of the concentration increment of individual component and consumed HONO normalized to CO in the daytime.

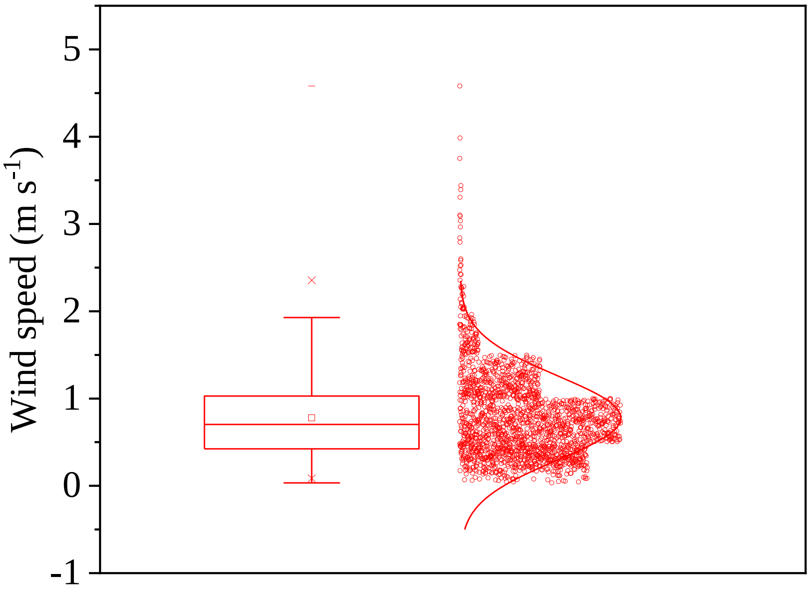

Figure S6. Distribution of wind speed when the $PM_{2.5}$ concentration was larger than 50 μg m^{-3} and the RH was less than 90 %.

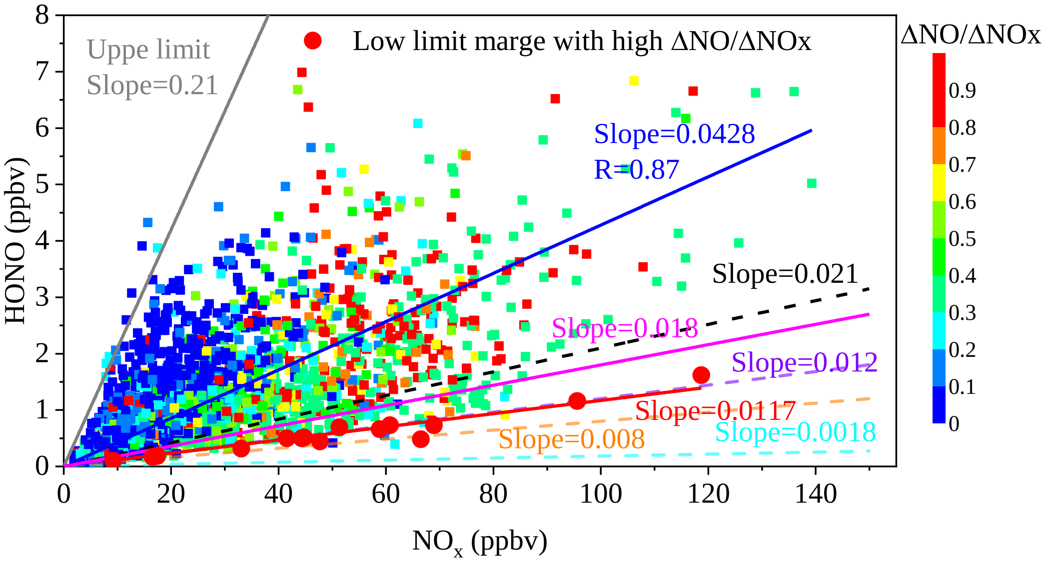

Figure S7. Correlation of measured HONO concentration with NO_x concentration.

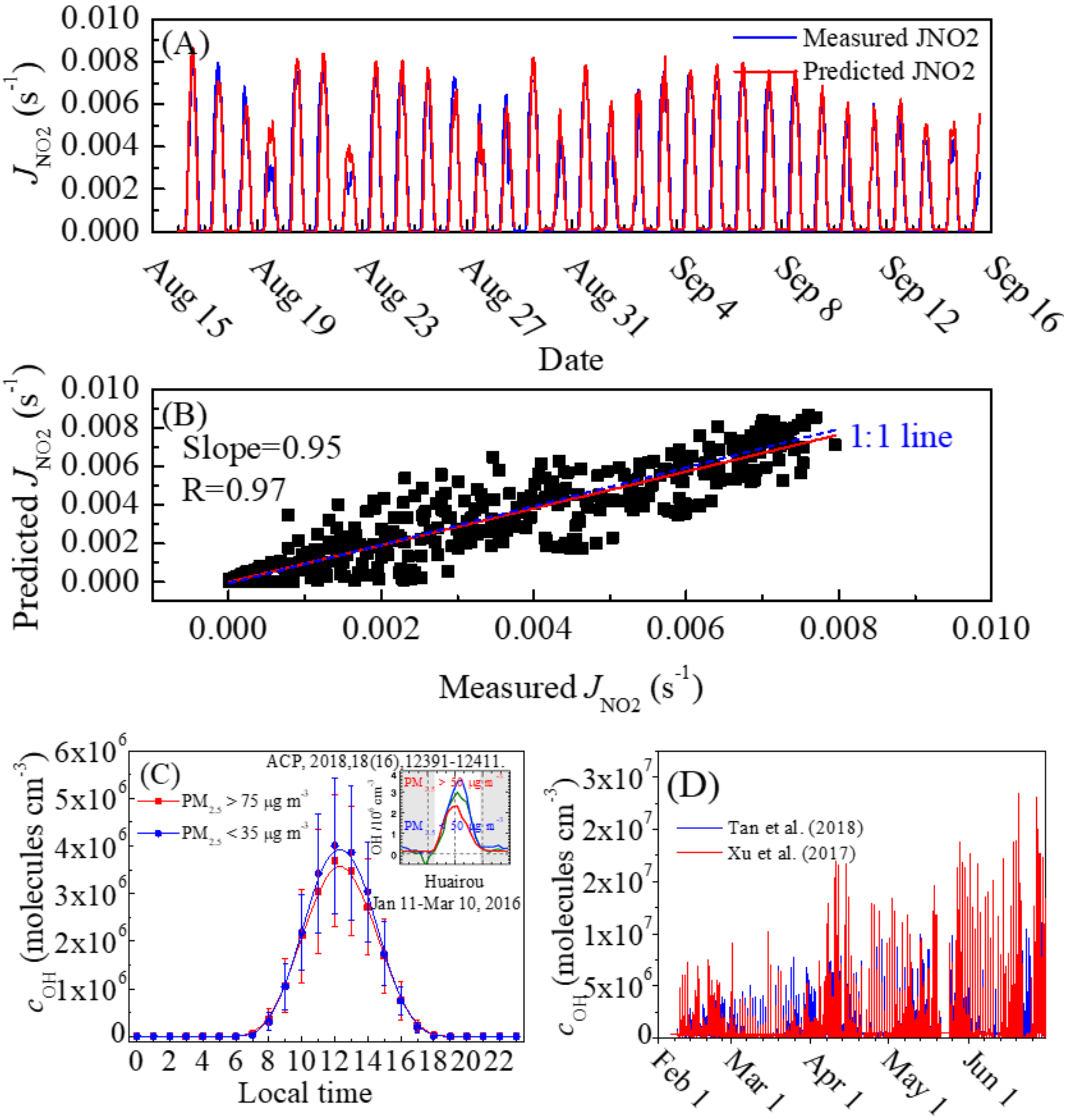

Figure S8. (A) Measured and predicted J_{NO2} and (B) the correlation between measured and predicted J_{NO2} from Aug. 15 to Sep. 16; (C) calculated diurnal curve of OH concentration based on J_{O1D} compared with that measured at Huairou (60 km northeast from BUCT) from Jan 11 to Mar 10, 2016; (D) Comparison of OH concentrations estimated using different methods.

Supplementary tables

Table S1. ANOVA statistics analysis for the monthly mean fraction of the individual component in NR-$PM_{2.5}$ and HONO concentration.

Component	Fraction of NR-$PM_{2.5}$ (%) or Concentration of gaseous pollutants (ppbv)	Feb	Mar	Apr	May
Ammonium	Feb (12.2±2.9)				
	Mar (14.2±2.8)	Significant			
	Apr (14.0±4.0)	Significant	Not significant		
	May (11.6±4.6)	Not significant	Significant	Significant	
	Jun (12.2±5.2)	Not significant	Significant	Significant	Not significant
Chloride	Feb (7.7±6.1)				
	Mar (4.4±2.6)	Significant			
	Apr (1.1±1.2)	Significant	Significant		
	May (0.7±1.1)	Significant	Significant	Not significant	
	Jun (0.3±0.2)	Significant	Significant	Significant	Not significant
Nitrate	Feb (16.2±8.5)				
	Mar (26.7±8.8)	Significant			
	Apr (22.0±11.7)	Significant	Significant		
	May (17.3±11.8)	Not significant	Significant	Significant	
	Jun (16.7±12.8)	Not significant	Significant	Significant	Not significant
Organic	Feb (47.9±10.7)				
	Mar (45.9±10.2)	Not significant			
	Apr (46.5±14.2)	Not significant	Significant		
	May (52.9±17.0)	Not significant	Significant	Significant	
	Jun (52.6±18.7)	Significant	Significant	Significant	Not significant

Sulfate	Feb (16.0±9.1)				
	Mar (8.8±5.4)	Significant			
	Apr (16.4±8.2)	Not significant	Significant		
	May (17.5±6.6)	Significant	Significant	Not significant	
	Jun (18.2±8.0)	Significant	Significant	Significant	Not significant
BC	Feb (3.0±2.8)				
	Mar (4.6±3.1)	Significant			
	Apr (3.2±2.6)	Not significant	Significant		
	May (2.8±2.1)	Not significant	Significant	Not significant	
	Jun (2.6±1.5)	Significant	Significant	Significant	Not significant
HONO	Feb (0.73±0.70)				
	Mar (1.53±1.25)	Significant			
	Apr (1.38±1.35)	Significant	Not significant		
	May (1.31±1.00)	Significant	Significant	Not significant	
	Jun (1.35±0.80)	Significant	Significant	Not significant	Not significant
NOx	Feb (20.4±17.3)				
	Mar (40.5±24.0)	Significant			
	Apr (22.8±18.6)	Not significant	Significant		
	May (25.0±15.9)	Significant	Significant	Not significant	
	Jun (19.0±12.1)	Not significant	Significant	Significant	Significant
SO_2	Feb (3.8±3.3)				
	Mar (12.1±13.0)	Significant			
	Apr (2.8±2.4)	Significant	Significant		
	May (1.8±1.7)	Significant	Significant	Not significant	
	Jun (1.3±1.2)	Significant	Significant	Significant	Not significant
CO	Feb (959.6±554.6)				

	Mar (1075.0±571.8)	Significant			
	Apr (546.6±378.1)	Significant	Significant		
	May (554.1±336.9)	Significant	Significant	Not significant	
	Jun (583.4±286.2)	Significant	Significant	Not significant	Not significant
	Feb (22.6±14.6)				
	Mar (23.8±19.2)	Not significant			
O_3	Apr (43.5±29.0)	Significant	Significant		
	May (42.5±28.3)	Significant	Significant	Not significant	
	Jun (57.2±30.7)	Significant	Significant	Significant	Significant

Note: "Significant" or "Not significant" denotes that the difference of the monthly mean fractions or concentrations is significant or not significant at the 0.05 level.

Tab. S2. Mean concentrations of HONO and $PM_{2.5}$ in selected episodes

Episode No.	Duration	HONO (ppb)	Average $PM_{2.5}$ concentration	NR-$PM_{2.5}$ Concentration (%)									
				Chloride		Nitrate		Organic		Sulphate		Ammonium	
				(%)	(μg m^{-3})	(%)	(μg m^{-3})	(%)	(μg m^{-3})	(%)	(μg m^{-3})	(%)	(μg m^{-3})
1	Feb 2-5	0.38±0.28	9.3±4.5	4.0±2.3	0.26±0.39	12.3±5.6	0.80±1.17	51.1±10.0	2.68±3.00	20.6±9.2	0.69±0.24	12.0±3.2	0.54±0.49
2	Feb 8-9	0.90±0.72	44.5±3.5	6.3±2.9	1.59±1.46	15.8±7.9	4.20±3.87	49.9±4.8	9.63±7.64	17.3±8.8	2.31±1.42	10.8±1.0	2.14±1.69
3	Feb 10-12	0.31±0.40	9.0±0.8	5.2±3.5	0.18±0.22	6.8±3.9	0.30±0.44	48.6±10.6	1.75±1.72	28.1±11.5	0.74±0.38	11.2±2.5	0.35±0.23
4	Feb 16-19	1.38±0.86	101.5±26.8	15.5±4.2	9.04±4.94	25.0±4.1	13.15±7.73	32.2±3.8	18.21±8.25	14.4±3.7	7.82±4.39	12.9±1.5	6.85±3.78
5	Feb 21-24	0.64±0.58	24.3±7.0	5.5±4.1	0.60±0.51	14.9±6.3	1.80±1.38	56.3±10.0	5.83±2.94	11.8±5.0	1.17±0.67	11.6±2.8	1.24±0.77
6	Feb 25-28	0.87±0.64	108.8±42.9	5.2±1.4	2.94±1.97	27.1±3.9	15.3±8.77	42.5±6.8	22.83±9.68	10.4±3.8	6.44±5.78	14.7±1.8	8.34±5.30
7	Mar 2-3	1.41±0.84	120.0±47.0	8.3±2.2	4.23±1.72	26.5±4.8	15.29±9.44	44.4±6.2	23.40±10.49	7.2±1.9	4.36±3.37	13.5±1.9	7.74±4.76
8	Mar 8-10	1.36±0.89	88.7±34.2	4.8±1.8	1.87±1.09	28.3±5.2	11.00±6.20	43.0±7.0	15.65±7.15	9.0±2.8	3.10±1.42	14.9±2.0	5.58±2.92
9	Mar 11-14	2.27±1.68	170.3±75.4	3.5±0.9	2.48±1.32	34.8±4.3	28.32±19.09	36.8±5.0	27.90±15.78	8.1±1.8	6.60±4.72	16.8±1.5	13.57±8.99
10	Mar 16-19	1.88±1.38	66.0±25.7	3.8±1.7	1.99±1.18	30.2±6.3	17.40±12.45	35.9±2.8	20.87±10.52	13.5±5.1	7.00±4.92	16.5±1.0	9.17±5.86
11	Mar 21-23	1.41±0.72	83.7±22.1	5.3±2.8	2.54±2.30	31.5±3.8	12.23±5.22	45.1±6.7	18.02±5.46	4.4±1.0	1.67±0.92	13.7±1.6	5.38±2.08
12	Mar 25-27	2.22±1.34	129.5±51.9	2.0±0.7	0.94±0.64	35.3±3.6	16.32±9.90	41.5±5.4	20.46±10.18	5.7±1.2	2.56±1.68	15.6±1.6	7.11±4.37

Table S3. The summary of the HONO/NOx ratio from vehicles in this study and the reported emission ratio of HONO/NOx from vehicles in China.

No.	Time	ΔNO/ΔNOx	$R_{\Delta NO/\Delta NOx}$	ΔHONO/ΔNOx	$R_{\Delta HONO/\Delta NOx}$
1	2018/2/6 5:00-8:00	1.00	0.99	1.3%	0.92
2	2018/2/8 5:00-8:00	0.94	0.99	1.8%	0.96
3	2018/3/3 5:00-8:00	0.98	0.99	2.4%	0.96
4	2018/3/13 5:00-8:00	1.00	0.99	1.4%	0.86
5	2018/4/15 5:00-7:00	0.82	0.97	2.3%	0.99
Mean		0.95±0.08	-	1.8±0.5%	-

Time	Place	Methods	ΔHONO/ΔNOx		Reference
			Range	Mean	
2015/9/1-2016/8/31	Ji'nan, Shandong	Empirical analysis of field data	0.19%-0.87%	0.53±0.20%	[5]
2011/8/3-2012/5/31	Hongkong	Empirical analysis of field data	0.5%-1.6%	1.2±0.4%	[6]
2014	Beijing	Tunnel experiment	-	2.1%	[7]
2017	Beijing	Chassis dynamometer	0.03%-0.42%	0.18%	[8]
2018/2/1-2018/6/30	Beijing	Empirical analysis of field data	1.3-2.4%	1.8±0.5%	This study
2018/2/1-2018/6/30	Beijing	Low limit correlation of field data	-	1.17±0.05%	This study

References:

1. Fröhlich, R.; Cubison, M. J.; Slowik, J. G.; Bukowiecki, N.; Prévôt, A. S. H.; Baltensperger, U.; Schneider, J.; Kimmel, J. R.; Gonin, M.; Rohner, U.; Worsnop, D. R.; Jayne, J. T., The ToF-ACSM: a portable aerosol chemical speciation monitor with TOFMS detection. *Atmos. Meas. Tech.* **2013,** *6*, (11), 3225-3241.
2. R. Williams, L.; A. Gonzalez, L.; Peck, J.; Trimborn, D.; McInnis, J.; R. Farrar, M.; Moore, K.; T. Jayne, J.; A. Robinson, W.; Lewis, D.; B. Onasch, T.; R. Canagaratna, M.; Trimborn, A.; Timko, M.; Magoon, G.; Deng, R.; Tang, D.; de la Rosa Blanco, E.; Prevot, A.; R. Worsnop, D., Characterization of an aerodynamic lens for transmitting particles greater than 1 micrometer in diameter into the Aerodyne aerosol mass spectrometer. *Atmos. Meas. Tech.* **2013,** *6*, 3271-3280.
3. Tong, S.; Hou, S.; Zhang, Y.; Chu, B.; Liu, Y.; He, H.; Zhao, P.; Ge, M., Exploring the nitrous acid (HONO) formation mechanism in winter Beijing: direct emissions and heterogeneous production in urban and suburban areas. *Faraday Discuss.* **2016,** *189*, 213-230.
4. Tan, Z. F.; Lu, K. D.; Jiang, M. Q.; Su, R.; Wang, H. L.; Lou, S. R.; Fu, Q. Y.; Zhai, C. Z.; Tan, Q. W.; Yue, D. L.; Chen, D. H.; Wang, Z. S.; Xie, S. D.; Zeng, L. M.; Zhang, Y. H., Daytime atmospheric oxidation capacity in four Chinese megacities during the photochemically polluted season: a case study based on box model simulation. *Atmos. Chem. Phys.* **2019,** *19*, (6), 3493-3513.
5. Li, D.; Xue, L.; Wen, L.; Wang, X.; Chen, T.; Mellouki, A.; Chen, J.; Wang, W., Characteristics and sources of nitrous acid in an urban atmosphere of northern China: Results from 1-yr continuous observations. *Atmos. Environ.* **2018,** *182*, 296-306.

6. Xu, Z.; Wang, T.; Wu, J.; Xue, L.; Chan, J.; Zha, Q.; Zhou, S.; Louie, P. K. K.; Luk, C. W. Y., Nitrous acid (HONO) in a polluted subtropical atmosphere: Seasonal variability, direct vehicle emissions and heterogeneous production at ground surface. *Atmos. Environ.* **2015,** *106*, 100-109.

7. Yang, Q.; Su, H.; Li, X.; Cheng, Y.; Lu, K.; Cheng, P.; Gu, J.; Guo, S.; Hu, M.; Zeng, L.; Zhu, T.; Zhang, Y., Daytime HONO formation in the suburban area of the megacity Beijing, China. *Sci. China-Chem.* **2014,** *57*, (7), 1032-1042.

8. Liu, Y.; Lu, K.; Ma, Y.; Yang, X.; Zhang, W.; Wu, Y.; Peng, J.; Shuai, S.; Hu, M.; Zhang, Y., Direct emission of nitrous acid (HONO) from gasoline cars in China determined by vehicle chassis dynamometer experiments. *Atmos. Environ.* **2017,** *169*, 89-96.